Development 137, 3603-3613 (2010) doi:10.1242/dev.049189

The *C. elegans* peroxidasin PXN-2 is essential for embryonic morphogenesis and inhibits adult axon regeneration

Jennifer R. Gotenstein[1], Ryann E. Swale[2], Tetsuko Fukuda[1], Zilu Wu[3], Claudiu A. Giurumescu[1], Alexandr Goncharov[3], Yishi Jin[3,4] and Andrew D. Chisholm[1,2,4,*]

SUMMARY

Peroxidasins form a highly conserved family of extracellular peroxidases of unknown cellular function. We identified the *C. elegans* peroxidasin PXN-2 in screens for mutants defective in embryonic morphogenesis. We find that PXN-2 is essential for specific stages of embryonic morphogenesis and muscle-epidermal attachment, and is also required postembryonically for basement membrane integrity. The peroxidase catalytic activity of PXN-2 is necessary for these developmental roles. *pxn-2* mutants display aberrant ultrastructure of the extracellular matrix, suggesting a role in basement membrane consolidation. PXN-2 affects specific axon guidance choice points in the developing nervous system but is dispensable for maintenance of process positions. In adults, loss of *pxn-2* function promotes regrowth of axons after injury, providing the first evidence that *C. elegans* extracellular matrix can play an inhibitory role in axon regeneration. Loss of function in the closely related *C. elegans* peroxidasin *pxn-1* does not cause overt developmental defects. Unexpectedly, *pxn-2* mutant phenotypes are suppressed by loss of function in *pxn-1* and exacerbated by overexpression of wild-type *pxn-1*, indicating that PXN-1 and PXN-2 have antagonistic functions. These results demonstrate that peroxidasins play crucial roles in development and reveal a new role for peroxidasins as extracellular inhibitors of axonal regeneration.

KEY WORDS: Epidermis, Extracellular matrix, Axon guidance, Genetic suppression, Leucine-rich repeat, Laser axotomy, *Caenorhabditis elegans*

INTRODUCTION

Peroxidasins are unusual secreted enzymes that contain both a peroxidase catalytic domain and multiple motifs found in extracellular matrix (ECM) proteins. The first peroxidasin was isolated biochemically from conditioned media of *Drosophila* Kc cells (Nelson et al., 1994). Most animal genomes encode at least one peroxidasin-like protein. The in vivo functions of peroxidasins have not been determined, although they have been proposed to act in basement membrane biogenesis, tissue development and innate immune defense (Nelson et al., 1994).

Peroxidasins contain an animal peroxidase catalytic domain (O'Brien, 2000). Animal peroxidases contain a heme group as a co-factor (Daiyasu and Toh, 2000; Furtmuller et al., 2006). The founding member of the animal peroxidase family is the neutrophil enzyme myeloperoxidase (MPO), which catalyzes the production of hypochlorous acid from hydrogen peroxide and chloride anion. Hydrogen peroxide is a relatively inert form of active oxygen and the action of MPO converts it into more reactive oxygen species with putative bactericidal roles. MPO is made in neutrophils, where it is either targeted to azurophilic granules or secreted extracellularly (Hansson et al., 2006). Expression of MPO by neutrophils is important for their function in innate immune defense against bacterial pathogens, and genetic MPO deficiency results in increased susceptibility to fungal infection in humans (Lehrer and Cline, 1969) and in a mouse model (Aratani et al., 1999). Other members of the animal peroxidase family, such as eosinophil peroxidase (EPO) and lactoperoxidase (LPO), are thought to have analogous roles in innate immune defense (Wang and Slungaard, 2006); the more distantly related thyroid peroxidase (TPO) functions in thyroid hormone synthesis (Ruf and Carayon, 2006). Several peroxidases may act as extracellular bactericidal agents in exocrine secretions (Ihalin et al., 2006).

As well as these established roles in innate immunity, peroxidases have been implicated in cell adhesion and formation of ECM. The extracellular oxidants generated by MPO can have both damaging and protective effects on the ECM (Rees et al., 2008), including inactivation of matrix metalloproteases (Wang et al., 2007) and formation of dityrosine cross-links (Heinecke et al., 1993). Other peroxidases are thought to promote cell-ECM adhesion. A crayfish cell adhesion protein was found upon purification to encode an MPO-like protein, named peroxinectin (Johansson et al., 1995). MPO itself promotes integrin-mediated adhesion of neutrophils (Johansson et al., 1997).

Among animal peroxidase domain-containing proteins, the peroxidasins are likely to be more stably associated with ECM because they are defined by the presence of other motifs typical of extracellular proteins, including leucine-rich repeats (LRRs) and immunoglobulin (Ig) domains. *Drosophila* Peroxidasin is expressed by blood cells (hemocytes) and some of their derivatives, such as plasmatocytes, and is deposited in basement membranes. Peroxidasin expression is widely used as a molecular marker for the early hemocyte lineage (Alfonso and Jones, 2002; Stofanko et al., 2008). Although the function of peroxidasin in *Drosophila* has not yet been assessed genetically, its expression in the blood cell lineage suggests that it could mediate some functions of blood cells. Hemocytes are migratory cells that deposit ECM and

[1]Section of Cell and Developmental Biology, Division of Biological Sciences, University of California San Diego, 9500 Gilman Drive, La Jolla, CA 92093, USA. [2]Department of Molecular, Cell and Developmental Biology, Sinsheimer Laboratories, University of California, Santa Cruz, CA 95064, USA. [3]Howard Hughes Medical Institute. [4]Section of Neurobiology, Division of Biological Sciences, University of California San Diego, 9500 Gilman Drive, La Jolla, CA 92093, USA.

*Author for correspondence (chisholm@ucsd.edu)

Accepted 25 August 2010

phagocytose dead or foreign cells. Hemocytes are crucial for a morphogenetic event known as condensation of the ventral nerve cord (VNC); if hemocyte migration is blocked, deposition of ECM components, including peroxidasin and type IV collagen, does not occur, leading to a failure of VNC condensation (Olofsson and Page, 2005).

To date, there has been no in vivo study of peroxidasin function. An amphibian peroxidasin is expressed during embryogenesis in specific organs, including the neural tube, otic vesicle, pronephros and tail-forming region (Tindall et al., 2005). By contrast, murine peroxidasin is more widely expressed (Homma et al., 2009). Human peroxidasin (*PXDN*) transcription is also widespread, whereas peroxidasin protein appears to be restricted to the cardiovascular system (Cheng et al., 2008). PXDN has been identified as a melanoma-associated antigen (Mitchell et al., 2000) and as a transcript that is upregulated in cells undergoing p53-induced apoptosis (Horikoshi et al., 1999). It is not yet known whether peroxidasin expression is functionally important in cancer or cell death.

The *C. elegans* genome encodes two highly related peroxidasins, PXN-1 and PXN-2. We show here that PXN-2 is essential for embryonic development and that it promotes basement membrane formation and maintenance of cell adhesion in postembryonic tissues. Adult *pxn-2* mutants display enhanced axon regrowth after injury, suggesting that PXN-2 contributes to an inhibitory microenvironment for regeneration in *C. elegans*. By contrast, PXN-1 is not essential for development. Unexpectedly, we find that PXN-1 and PXN-2 have antagonistic roles in development, revealing complexity in the functions of this family of extracellular enzymes.

MATERIALS AND METHODS

Genetics and strain construction

C. elegans strains were maintained on NGM agar plates at 20-22°C following standard procedures. Bristol N2 was used as wild type for all crosses and scoring. In addition to the *pxn* mutants described below, we used the following mutations: *dpy-7(e88)*, *unc-9(e111)*, *spon-1(ju430*ts*)*, *rrf-3(pk1426)*, *nDf19*; and transgenes P*unc-25*-GFP (*juIs76*), P*acr-2*-GFP (*juIs14*) (Huang et al., 2002), P*mec-4*-GFP (*zdIs5*), P*tph-1*-GFP (*zdIs13*) (Clark and Chiu, 2003), P*sra-6*-GFP (*oyIs14*), P*myo-3*-memYFP (*trIs10*) (Dixon et al., 2006), HIM-4::GFP (*rhIs23*) (Vogel and Hedgecock, 2001) and MUP-4::GFP (*juIs172*) (Hong et al., 2001).

The *pxn-2* mutations *ju328*, *ju358*, *ju379*, *ju403*, *ju432*, *ju436* and *ju445* were isolated in a semi-clonal screen for ethyl methanesulfonic acid (EMS)-induced mutants with defects in embryonic elongation and muscle detachment (M. Ding, W.-M. Woo and A.D.C., unpublished). *pxn-2(tm3464)*, provided by S. Mitani (Tokyo Women's Medical University), comprises a 630 bp deletion and a 6 bp insertion and is predicted to result in deletion of residues Q748 to K877 and termination of translation in the peroxidase domain. *pxn-1(ok785)* is a 1084 bp deletion predicted to cause a frameshift at D473 in the second Ig domain of PXN-1, followed by a premature stop codon. *ok785*-containing strains were genotyped using multiplex PCR. In complementation tests for lethal mutations, or to generate *pxn-2/Df* heterozygotes, we used *tra-2(q122*dm*)* to feminize hermaphrodites and *tra-2(q276)* to generate XX pseudomales.

Mapping, transgenic rescue, RNA interference and sequencing

We mapped *ju432* between *dpy-7* and *unc-9* by three-factor mapping. We further mapped *ju432* using the polymorphic strain CB4856 (Wicks et al., 2001) to a 157 kb region between SNPs F47B10[2] and CE6-1202. Extrachromosomal arrays containing cosmid K09C8 (*juEx1044*, *juEx1045*) fully rescued the morphology and lethality defects of *pxn-2* mutants (not shown). We performed RNA interference (RNAi) on the four largest genes in the K09C8 region and found that RNAi of K09C8.5/*pxn-2* phenocopied the *ju432* phenotypes, when performed in the sensitized *rrf-3* or *eri-1* backgrounds, but not in N2. We confirmed the *pxn-2* gene structure by sequencing cDNAs yk448b10 and yk643e10. The *pxn-2* transcript extends over 7.1 kb, contains 21 exons, and encodes a 1328 amino acid polypeptide of a predicted 151 kDa. To identify the molecular lesions of *pxn-2* alleles we amplified mutant DNAs by PCR and sequenced them at the UC Berkeley DNA Sequencing Facility. For feeding RNAi of *lam-3* we used Ahringer library clone I-5G24 (Kamath et al., 2003).

Phenotypic analysis

We quantitated the penetrance of lethal and epidermal morphology defects as previously described (George et al., 1998). We collected time-lapse differential interference contrast (DIC) 'four-dimensional' (4D) movies as described (Hudson et al., 2006). At least ten embryos were recorded per genotype. We scored muscle detachment and axon guidance as described (Woo et al., 2008). Drug sensitivity and egg-laying assays followed standard procedures (Hart, 2006). All drugs were obtained from Sigma. Statistical tests used Prism (GraphPad, La Jolla, CA).

For electron microscopy, we fixed worms using high-pressure freezing and freeze substitution in tannic acid and osmium in acetone, as described (Weimer, 2006). Five *ju432* and six L4 stage *ju358* animals were fixed and sectioned in the head and anterior body regions. Femtosecond laser axotomy was performed with the laser in MHz mode, as described (Wu et al., 2007).

Molecular biology and transgenes

To generate *pxn-2* transcriptional reporters we amplified 1.8 kb 5′ to the *pxn-2* ATG by PCR (see Table S1 in the supplementary material) and linked it to a GFP fragment amplified from plasmid pPD95.75 using duplex PCR (Hobert, 2002). The resulting PCR products were injected at 50 ng/μl with the co-injection marker P*ttx-3*-RFP (Hobert et al., 1997) to generate transgenes *juEx1060-1063*; all four displayed indistinguishable expression. P*pxn-1*-GFP transcriptional reporters *juEx1100* and *juEx1101* (in Fig. 7B) were made using duplex PCR, amplifying 3 kb 5′ to the *pxn-1* ATG. Confocal images and time-lapse movies were taken on a Zeiss LSM510 confocal microscope and processed with Zen Software.

A near full-length *pxn-2* cDNA, yk643e10, was kindly provided by Y. Kohara (National Institute of Genetics, Mishima, Japan). yk643e10 contains the entire ORF except for the first 25 bp. The P*pxn-2*-PXN-2 cDNA minigene pCZ792 was generated by inserting the 1.8 kb *pxn-2* promoter fragment into yk643e10, using *Not*I and *Dra*III sites introduced by PCR. pCZ792 was injected at 1 ng/μl (*juEx2142*), 5 ng/μl (*juEx2163*) and 50 ng/μl (*juEx2140*), all with P*ttx-3*-RFP.

To generate YFP-tagged PXN-2 we used Gateway cloning (Invitrogen) to insert a PXN-2 cDNA lacking its N-terminal signal sequence into the vector pCZGY20, which contains the KAL-1 secretion signal sequence followed by Venus YFP (Hudson et al., 2006). We then inserted the 1.8 kb *pxn-2* promoter to create P*pxn-2*-YFP::PXN-2 (pCZGY926). pCZGY926 was injected at 50 ng/μl with the P*ttx-3*-RFP marker to generate arrays *juEx2492-2495*; images in Fig. 3 are of *juEx2492*. To visualize YFP expression we used anti-GFP immunostaining, as described (Woo et al., 2008). To overexpress PXN-2 we injected pCZGY926 at 100 ng/μl and generated arrays *juEx2908-2910*. Unlike most *juEx2492* embryos, embryos transgenic for these high-concentration arrays displayed YFP fluorescence visible under the dissection microscope.

For site-directed mutagenesis we used the QuikChange Kit (Stratagene) or religation of digested plasmids from the P*pxn-2*-PXN-2 cDNA minigene (pCZ792). The following clones and transgenic lines were generated: pCZ794 (H755A: *juEx2490*, *juEx2491*), pCZ795 (ΔLRR, deletion of residues 26-208; *juEx2540*, *juEx2543-2545*), pCZ797 (ΔIg, residues 293-602; *juEx2541-2542*). We confirmed all constructs by sequencing and injected them at 25-50 ng/μl to create transgenes. YFP-tagged versions of the H755A and ΔIg clones were created by subcloning the mutated regions into pCZGY926. The resulting clones were injected at 50 ng/μl to create *juEx2898* [YFP::PXN-2(H755A)] and *juEx2899* (YFP::PXN-2ΔIg).

To overexpress *pxn-1* we injected the *pxn-1(+)* fosmid clones WRM0616aF08 and WRM0621bE07 at 25-30 ng/μl with P*ttx-3*-RFP to create *juEx2911-2914* and *juEx2915*, respectively.

To generate transgenes in which the PXN-2 peroxidase domain had been replaced with that of PXN-1, we amplified exons coding for the *pxn-1* peroxidase domain and cloned them into the YFP::PXN-2 clone pCZGY926. Using restriction sites introduced by the PCR we cloned *pxn-1* peroxidase domain genomic DNA fragments into pCZGY926 cut with *Msc*I and either *Mlu*I or *Sbf*I to generate pCZGY1104 and pCZGY1105, respectively. The resulting transgenes are predicted to encode PXN-2::PXN-1 chimeric proteins consisting of the first 652 residues of PXN-2, 506 residues of PXN-1 peroxidase domain and the last 170 residues of PXN-2 (*Mlu*I, pCZGY1104), or the first 652 residues of PXN-1, 643 PXN-1 residues comprising the entire peroxidase domain and most of the C-terminus apart from the final 20 residues of PXN-2 (*Sbf*I, pCZGY1105). These constructs were injected at 50 ng/μl to generate *juEx2900-2903* (pCZGY1104) and *juEx2904-2907* (pCZGY1105) with the P*ttx-3*-RFP co-injection marker.

RESULTS

The peroxidasin PXN-2 is essential for *C. elegans* embryonic development

Elongation is the final major stage of *C. elegans* embryonic morphogenesis (Chisholm and Hardin, 2005). Elongation is driven by active rearrangement of the epidermal cytoskeleton (Priess and Hirsh, 1986) and the contraction of underlying muscles, transduced via intervening ECM (Williams and Waterston, 1994). Loss of function in certain basement membrane components, such as SPON-1 (Woo et al., 2008), disrupts late stages of elongation due to progressive loss of adhesion between body wall muscles and the epidermis. To identify additional components of the embryonic ECM we performed semi-clonal screens for lethal mutations with this set of defects. Among the 40 mutations identified in this screen, we mapped seven to a small region of the X chromosome and found that they form a single complementation group. We identified the gene affected by these mutations as *pxn-2*, which encodes a member of the peroxidasin family of putative extracellular peroxidases (Fig. 1A-C).

The *pxn-2* alleles isolated in our screen form an allelic series, which in order of decreasing phenotypic strength are *ju379*, *ju445*>*ju358*>*ju432*>*ju403*>*ju328*>*ju436* (Table 1). A *pxn-2* deletion mutation, *tm3464* (kindly provided by S. Mitani), resembles *ju379* and *ju445* in phenotype (see below). Semi-viable *pxn-2* alleles cause similar defects, including variably abnormal epidermal morphology (the Vab phenotype), detachment of body muscles from the epidermis (Mua), defective egg laying (Egl) and reduced brood size (Table 1). The mutations *ju379*, *ju445* and *tm3464* cause fully penetrant embryonic and early larval lethality (Fig. 1D; see below). The lethal and morphological phenotypes of *pxn-2* mutants were fully rescued by transgenes containing either *pxn-2* genomic DNA (not shown) or a full-length *pxn-2* cDNA expressed under the control of a 1.8 kb *pxn-2* promoter (Fig. 1D).

Peroxidasins are secreted proteins that contain several LRRs, two to four Ig domains and a heme peroxidase catalytic domain (Fig. 1B). The PXN-2 peroxidase domain contains all the key residues required for heme coordination and catalytic activity (Zamocky et al., 2008), and is 52% identical to the peroxidase domain of murine peroxidasin (Q3UQ28) and 50% identical to that of *Drosophila* peroxidasin. Overall, PXN-2 is most closely related to its ortholog in *C. briggsae* (CBG15737), followed by the other *C. elegans* peroxidasin, PXN-1 (see below).

Three *pxn-2* mutants carry missense alterations in the peroxidase domain: the strongest viable allele, *ju358*, affects a non-conserved glutamate; *ju328* affects a conserved arginine; and *ju436* affects a semi-conserved histidine. The relatively minor change (R to K) in a side chain due to *ju328* may account for the comparatively weak effect of changing this conserved residue. To test whether the peroxidase catalytic activity of PXN-2 is important for its developmental functions, we mutated the 'distal histidine' of the peroxidase active site to alanine (H755A). Mutation of the equivalent residue in MPO completely abolishes catalytic activity without affecting protein stability (Jacquet et al., 1994). PXN-2(H755A) transgenes displayed significantly reduced rescue activity compared with wild-type PXN-2 transgenes (Fig. 1D), indicating that peroxidase catalytic activity is crucial for PXN-2 developmental functions. PXN-2 transgenes lacking either the LRRs or the Ig domains failed to rescue *pxn-2* mutants (not shown).

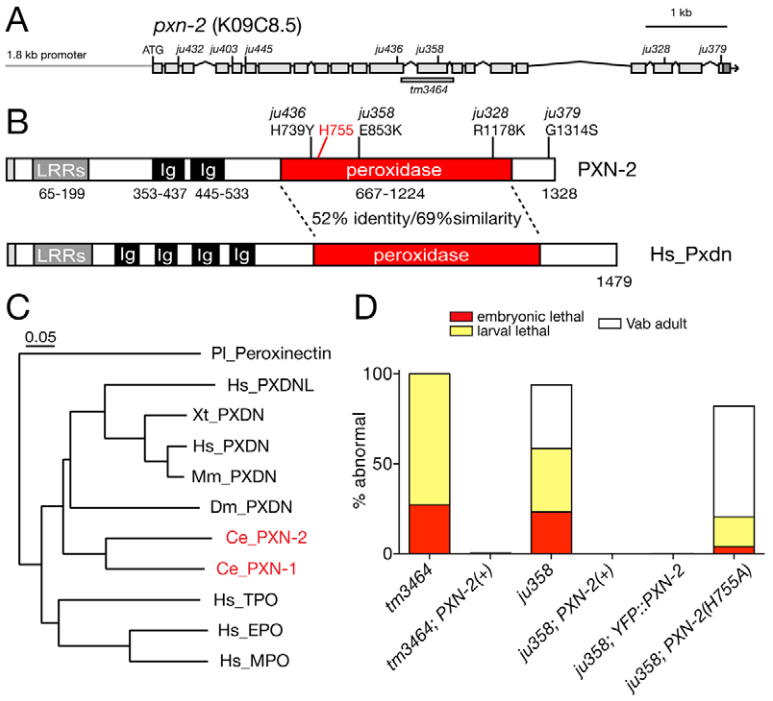

Fig. 1. *pxn-2* encodes a *C. elegans* peroxidasin that is required for body morphogenesis. (**A**) Genomic structure of *pxn-2*, showing locations of point mutations and the *tm3464* deletion. (**B**) Domain organization of PXN-2 and human (Hs) peroxidasin. (**C**) *C. elegans* PXN-2 and PXN-1 are most closely related to *Drosophila* and vertebrate peroxidasins, and more distantly related to other myeloperoxidases. Neighbor-joining tree based on ClustalW alignment of peroxidase domains. Ce, *C. elegans*; Dm, *Drosophila melanogaster*; Pl, *Pacifastacus leniusculus* (crayfish); Xt, *Xenopus tropicalis*; Mm, *Mus musculus*; Hs, *Homo sapiens*. Humans have two peroxidasin-encoding genes, *PXDN* and *PXDNL*; however, phylogenetic analysis indicates that the two *C. elegans* peroxidasins diverged separately and are not orthologous to the vertebrate gene pairs. (**D**) Morphological and lethal phenotypes of *pxn-2(tm3464)* and *pxn-2(ju358)* are completely rescued by transgenes containing a *pxn-2* cDNA under the control of a 1.8 kb *pxn-2* promoter [PXN-2(+), *juEx2140*] and by the YFP::PXN-2 transgene (*juEx2492*). Rescue activity of PXN-2(H755A) transgenes (*juEx2491*) was significantly reduced compared with that of PXN-2(+). Vab, variably abnormal epidermal morphology phenotype.

Table 1. *pxn-2* allelic series and DNA lesions

Allele	Embryonic lethal (%)	Larval lethal (%)	Adult Vab (%)	Adult non-Vab (%)	DNA change	Predicted effect
ju436	0.3	0	20.0	79.7	CAT→TAT	H739Y
ju328	2.5	2.5	23.7	71.3	AGA→AAA	R1178K
ju403	4.6	21.7	66.1	7.6	cagCTT→caaCTT	Exon 6 splice acceptor
ju432	12.5	16.1	33.5	37.9	GAGgta→GAGata	Exon 2 splice donor
ju358	31.1	46.8	21.2	0.9	GAA→AAA	E853K
ju379/+	6.0	13.7	0	(80.3)	GGC→AGC	G1314S
ju445/+	5.2	15.2	0	(79.5)	aagAAT→aaaAAT	Exon 5 splice acceptor
tm3464/+	4.25	11.8	0	(83.6)	630 bp deletion	Premature stop codon

Penetrance of lethal and morphological phenotypes was determined from counts of several complete broods (*n*>500 progeny for each genotype). Mutant strains are homozygous viable with the exception of *ju379*, *ju445* and *tm3464*.

PXN-2 promotes late embryonic elongation and muscle attachment

Approximately 25-30% of animals mutant for the strong alleles *ju379*, *ju445* and *tm3464* arrested as unhatched eggs; the remainder hatched and arrested as incompletely elongated L1 larvae. To define when *pxn-2* acts in morphogenesis we used time-lapse recordings in multiple focal planes (4D movies). Most *pxn-2(tm3464)* and *pxn-2(ju445)* mutants developed normally until just after the twofold stage of epidermal elongation (Fig. 2A,B). For *tm3464* embryos, 7/11 displayed normal muscle contractions starting at the 1.75-fold stage and elongated to twofold. Within ~15 minutes of reaching the twofold stage, the embryos developed deformities in the epidermis; elongation continued with decreased muscle twitching until the embryos arrested at ~2.5-fold elongation. Other embryos ceased elongation at the threefold stage. The deficiency *nDf19* failed to complement *pxn-2*; embryos of genotype *pxn-2(tm3464)/nDf19* (see Materials and methods) mostly resembled *tm3464* homozygotes, suggesting that *tm3464* eliminates *pxn-2* function. A small fraction of *ju379* or *tm3464/Df* embryos displayed morphological defects before the twofold stage, suggesting that PXN-2 might play a minor role in earlier elongation. Most *ju379* embryos elongated to the threefold stage before arresting; *pxn-2(ju432)* mutants displayed milder defects than those of the lethal alleles, beginning in late elongation after the threefold stage. We conclude that PXN-2 function becomes critical soon after the twofold stage of epidermal elongation.

The defects of *pxn-2* embryos most closely resemble those of animals lacking the basement membrane components type IV collagen (EMB-9/LET-2) or F-spondin (SPON-1) (Gupta et al., 1997; Woo et al., 2008). Unlike animals lacking integrins or perlecan, muscle development appeared initially normal in *pxn-2* mutants. Perlecan itself displayed normal localization to muscle quadrants, developing gaps in later elongation after muscle detachment (Fig. 2D). *pxn-2* mutants also displayed normal localization of laminin (not shown), suggesting that PXN-2 is not required for the initial stages of basement membrane assembly. We

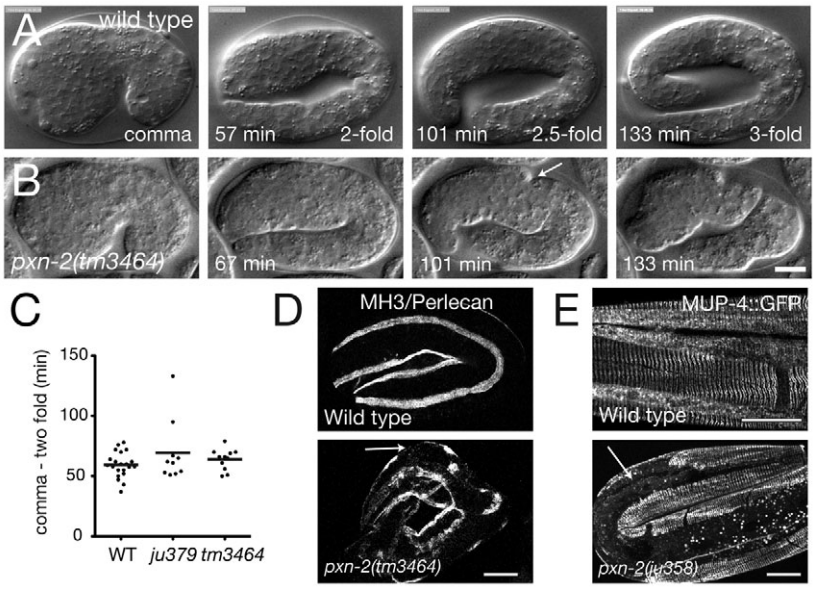

Fig. 2. *pxn-2* mutant embryos are defective in late stages of epidermal elongation, in muscle attachment and in epidermal attachment structures. (**A**,**B**) Frames from 4D Nomarski DIC movies of embryogenesis in wild-type N2 (A) and *pxn-2(tm3464)* (B) *C. elegans* embryos. Elongation proceeds normally until the twofold stage in *pxn-2* mutants. Between 20 and 40 minutes after the twofold stage, visible constrictions appear in the epidermis (arrow), and elongation ceases ~1 hour later, in most cases not extending to the threefold stage. (**C**) Early elongation rates are normal in *pxn-2* mutants. Dot plot of times from comma stage to twofold as measured in time-lapse movies. Horizontal lines indicate the mean. WT, wild type. (**D**) In wild-type embryos, perlecan (UNC-52) (MH3 immunostaining) is localized to the basement membrane of muscle quadrants. In threefold *pxn-2(tm3464)* embryos this localization is retained except where muscles have detached from the epidermis, leaving gaps in the perlecan-staining bands (arrow). (**E**) In the wild-type larvae, MUP-4::GFP is localized to regularly spaced attachment structures in the epidermis. In *pxn-2* mutant larvae, MUP-4::GFP is absent from regions of muscle detachment (arrow). Scale bars: 10 μm.

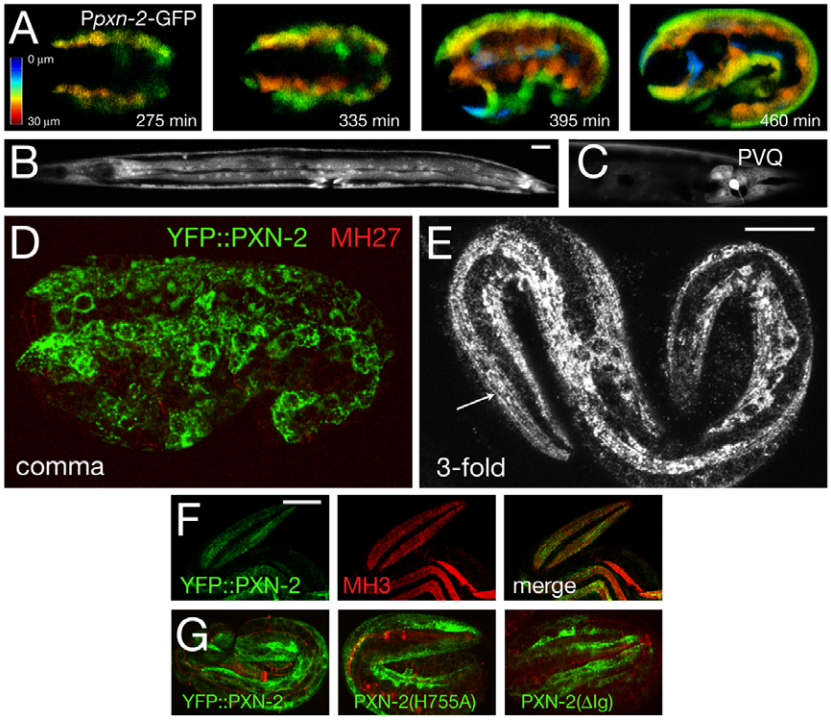

Fig. 3. *pxn-2* is expressed in embryonic and larval epidermis and in selected neurons. (**A**) The P*pxn-2*-GFP transcriptional reporter (*juEx1061*) is expressed in epidermal cells from late gastrulation (~210 minutes after the first cleavage) onward. Images are depth-coded projections of confocal *z*-stacks of a single *C. elegans* embryo imaged over time. (**B**) P*pxn-2*-GFP expression in epidermis and vulval muscles at the L4 stage. (**C**) P*pxn-2*-GFP is expressed in the PVQ neurons in postembryonic stages. P*pxn-2*-GFP is also expressed in the BDU neurons and in four neurons in the anterior ventral ganglion (not shown). (**D**,**E**) Expression of functional YFP::PXN-2 (*juEx2492*) in embryos. Anti-GFP immunostaining (green) and MH27 (anti-AJM-1) staining (red). (D) At comma stage, YFP::PXN-2 is predominantly intracellular in epidermal cells. Maximum transparency projection of confocal sections (7 × 0.3 µm). (E) At the threefold stage, YFP::PXN-2 appears partly extracellular, forming faint longitudinal striations along the quadrants of body wall muscles (arrow). Projection of two confocal sections, 0.3 µm apart. (**F**) Colocalization of YFP::PXN-2 (green) and perlecan (MH3 immunostaining, red) in the threefold embryo; single confocal section. (**G**) Equivalent confocal projections of threefold stage embryos transgenic for YFP::PXN-2 (*juEx2492*), YFP::PXN-2(H755A) (*juEx2898*) and YFP:: PXN-2(ΔIg) (*juEx2899*). Images are projections of 6 × 0.5 µm focal planes in the top 3 µm. Scale bars: 10 µm.

infer that a weakened muscle-epidermal basement membrane attachment is broken by the force of muscle contraction, leading to defects in the epidermal cytoskeleton and subsequent failure to elongate. Indeed, in larvae, regions of detached muscle correlated with gaps in the pattern of epidermal cytoskeletal attachment structures, as visualized by components such as MUP-4 (Hong et al., 2001) (Fig. 2E), suggesting that muscle detachment results in local disorganization of the epidermal cytoskeleton.

pxn-2 is expressed in epidermal cells from early embryogenesis onwards

pxn-2 transcriptional GFP reporters containing the 1.8 kb promoter sequence defined by rescue experiments (Fig. 1D) were expressed in the embryonic epidermis (Fig. 3). Expression was observed in epidermal precursors beginning in late gastrulation (~200 minutes after the first cleavage), which is ~4 hours before the elongation defects of *pxn-2* mutants become apparent at 450 minutes (Fig. 3A). P*pxn*-2-GFP was expressed by most differentiated epidermal cells throughout embryonic, larval and adult development (Fig. 3B). In adults, P*pxn-2*-GFP was expressed in vulval muscles (Fig. 3B) and in a small number of neurons, including PVQ (Fig. 3C).

To determine where PXN-2 protein is localized, we generated YFP-tagged PXN-2 transgenes. These transgenes fully rescued *pxn-2(ju358)* (Fig. 1D) and *pxn-2(tm3464)* (not shown), indicating that the YFP tag does not disrupt PXN-2 function. As with the *pxn-2* transcriptional reporters, GFP::PXN-2 was expressed in epidermal cells at all stages, in vulval muscles and in a few neurons. In early embryonic epidermal elongation, most YFP::PXN-2 appeared to be intracellular in epidermal cells, in the locations that likely correspond to compartments of the secretory pathway (Fig. 3D). By late elongation, YFP::PXN-2 was also found in longitudinal striations adjacent to body wall muscle quadrants (Fig. 3E). As such longitudinal structures are not found inside the epidermis these are likely to represent localization to the basement membrane between the epidermis and muscles. Consistent with this interpretation, YFP::PXN-2 localized close to endogenous basement membrane components such as perlecan (Fig. 3F). In larval and adult stages, YFP::PXN-2 was faintly visible throughout the epidermis, in vulval muscles and in PVQ neurons (not shown). Transgenes expressing YFP::PXN-2(H755A) and YFP::PXN-2(ΔIg) were made by injection at the same concentration as wild-type YFP::PXN-2. Mutant fusion proteins were expressed within epidermal cells and showed a range of localization similar to the wild-type protein (Fig. 3G). Like the wild-type protein, some YFP-tagged PXN-2 accumulated within the epidermis; however, some punctate or striated staining, similar to that in the wild type, was also observed. These observations suggest that the failure of the H755A and ΔIg transgenes to rescue is likely to be due to the requirement for peroxidase activity and the Ig domains for proper PXN-2 function. However, we cannot exclude the possibility that improper localization or processing also contributes to the failure to rescue.

PXN-2 maintains postembryonic cell-matrix adhesion of body muscles and pharyngeal cells

C. elegans body wall muscles are attached to the epidermis via a basement membrane between the two tissues. *pxn-2* mutants displayed a progressive detachment of body muscles from the epidermis during larval development (Fig. 4A,B). To test whether forces due to body muscle contraction were causing progressive detachment, we paralyzed muscles using levamisole and found that this significantly suppressed muscle-epidermal and muscle-muscle detachment in *pxn-2(ju432)* (Fig. 4B). This result implies that the muscle-epidermal and muscle-muscle detachment defects of *pxn-2* mutants are in part due to a failure to maintain strong adhesive attachments. Levamisole suppressed epidermal morphology defects in the stronger mutant *ju358*, but only slightly suppressed muscle detachment (Fig. 4B). The inability of levamisole to significantly suppress detachment defects in *ju358* mutants might be because in this more severe mutant the body muscles have become irreversibly detached during embryogenesis.

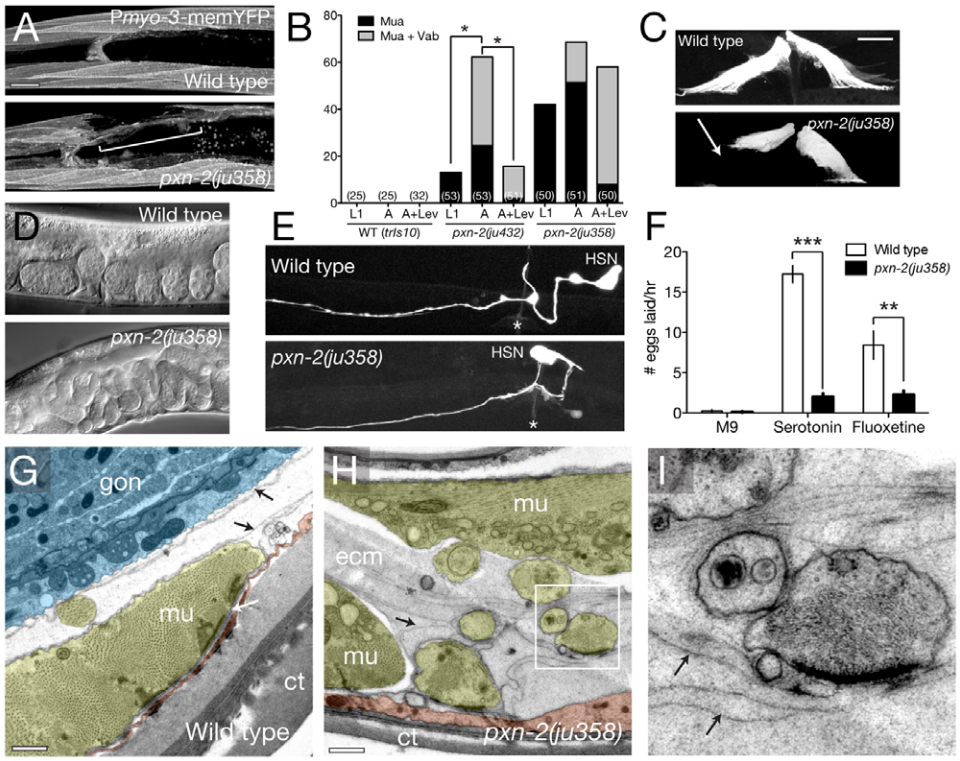

Fig. 4. PXN-2 maintains postembryonic muscle-epidermal adhesion and promotes ECM consolidation. (**A**) Anterior body wall muscle morphology in wild-type (*trls10*) and *pxn-2(ju358) C. elegans* embryos. A region of muscle detachment in *pxn-2(ju358)* is bracketed. Projections of confocal *z*-stacks. (**B**) The muscle attachment (Mua) phenotype in *pxn-2(ju432)* is progressive in larval development and can be suppressed by paralysis with levamisole. *pxn-2(ju358)* causes more penetrant Mua phenotypes at the L1 stage; these are slightly progressive and are not significantly reduced by paralysis. The number of animals scored in each column is indicated in parentheses. *, $P<0.05$; Fisher's exact test. (**C**) Vulval muscles in the wild type are symmetrically attached, whereas in *pxn-2* mutants the muscles become detached (arrow); P*egl-15*-GFP (*ayIs2*). (**D**) *pxn-2* animals exhibit the defective egg laying (Egl) phenotype. (**E**) In the wild type, the HSN cell body is located posterior to the vulva (asterisk) and extends an axon to the vulval epithelium. In ~25% of *ju358* or *ju432* (not shown) adults, the HSN cell body is anterior to its normal position; P*tph-1*-GFP (*zdIs13*). (**F**) Wild-type animals are inhibited from egg laying in liquid (M9 buffer); this inhibition is overcome by serotonin (35 mM) or the serotonin re-uptake inhibitor fluoxetine (1 mg/ml). Serotonin or fluoxetine only weakly stimulate egg laying in *pxn-2(ju358)* mutants. **, $P<0.01$; ***, $P<0.001$; Student's *t*-test. (**G-I**) Ultrastructure of the muscle-epidermal ECM is aberrant in *pxn-2(ju358)* animals. In the wild type (G), body wall muscles (mu, yellow) are attached to the epidermis (red) and cuticle (ct) via a basement membrane (white arrow); basement membranes covering the internal muscle surface and the gonad (gon, blue) are also visible (black arrows). (H) In *pxn-2(ju358)* mutants, the body muscles are separated from the epidermis and sometimes surrounded by expanded extracellular material (ecm) containing multiple electron-dense laminae of similar thickness to normal basement membranes (black arrows). (I) Enlargement of boxed region in H, showing muscle finger surrounded by laminae (arrows). Scale bars: 10 μm in A,C; 500 nm in G,H.

pxn-2 mutant adults also displayed highly penetrant defects in egg laying (Fig. 4C). In wild-type hermaphrodites, eggs are expelled by contractions of vulval muscles attached to the epidermis and uterus; vulval muscle contraction is stimulated by serotonergic HSN neurons (Schafer, 2006). Although HSN neurons were occasionally mispositioned in *pxn-2* mutants (Fig. 4D), the primary cause of the Egl defect appears to be a defective attachment of vulval muscles (Fig. 4E). Consistent with this interpretation, the *pxn-2* Egl phenotype was only marginally suppressed by treatment with exogenous serotonin or serotonin re-uptake inhibitors (Fig. 4F).

To test whether the muscle detachment phenotypes of *pxn-2* mutants reflect a defect in the basement membrane, we examined ECM ultrastructure. Muscles and epidermal cells normally generate basement membranes that are 20-100 nm thick (Fig. 4H,G) (Kramer, 2005). By contrast, in *pxn-2* mutants, we often observed a diffuse, apparently unstructured ECM within which were embedded multiple electron-dense basement-membrane-like layers (Fig. 4H). These expanded matrices filled the body cavity between the muscle, VNC, epidermis and intestine, although the integrity of the intestinal and gonadal basement membranes appeared normal. Within the expanded matrix muscle cells were extended finger-like projections with membrane plaques resembling those of dense bodies (Fig. 4I).

pxn-2 mutants also displayed striking progressive defects in the morphology of the adult pharynx. Over the course of several days the shape of the anterior pharyngeal bulb became progressively distorted (Fig. 5A). ECM component HIM-4 (hemicentin) is normally localized to the pharyngeal basement membrane and tracks that tether the anterior pharynx to the epidermis (Fig. 5B). In *pxn-2* mutants, HIM-4 distribution was highly abnormal around the pharynx and formed large inclusions instead of linear tracks (Fig. 5B). The pharyngeal basement membrane itself was also aberrant (Fig. 5C,D), resembling the unstructured material seen near body wall muscles.

To further address whether PXN-2 promotes basement membrane function we tested whether reduction of *pxn-2* function could sensitize animals to loss of function in other known basement membrane components. We grew *pxn-2(ju432)* worms on bacteria expressing dsRNA for laminin αA (encoded by *lam-3*) (Huang et al.,

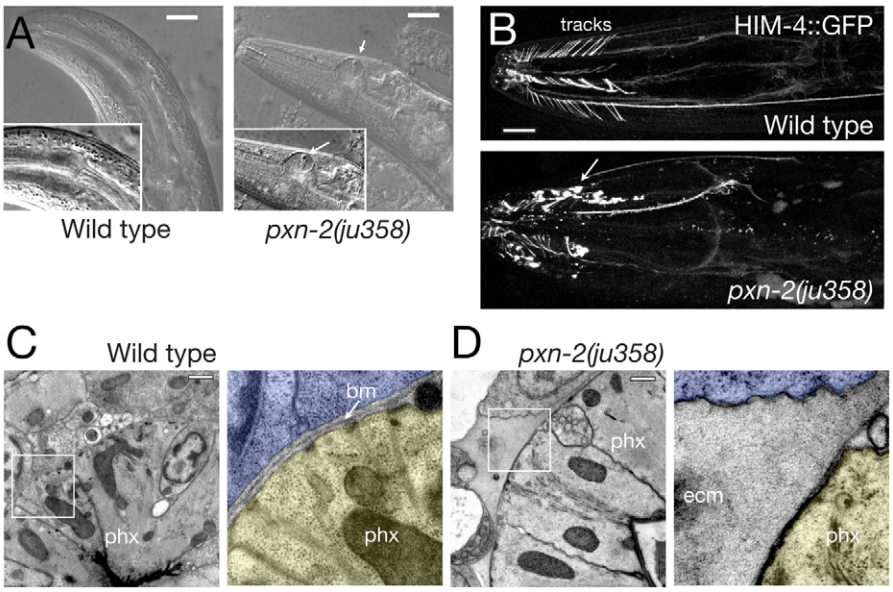

Fig. 5. *pxn-2* adults display progressive distortion of the pharynx and disorganization of pharyngeal ECM. (**A**) Deformation of the anterior pharyngeal bulb in *pxn-2(ju432)* adult *C. elegans* (DIC images). Vacuoles (white arrows) are frequently seen around the pharyngeal region, possibly resulting from cell necrosis. (**B**) Progression of pharyngeal distortion in a single *pxn-2(ju358)* adult. The pharynx morphology defects increase in penetrance during adult life: 19% of day 1 adult *ju358* animals displayed overt pharyngeal defects, whereas 69% of day 5 adult *ju358* animals displayed defects (n>50 per time point). In the wild type, HIM-4::GFP (*rhIs23*) is present on the pharyngeal basement membrane and in flexible tracks connecting the anterior pharynx to the epidermis. In *pxn-2(ju358)*, HIM-4::GFP accumulates in extracellular aggregates (arrow). (**C**) Electron micrographs showing pharyngeal basement membrane (bm) in the wild type. In the enlargement (right), the pharynx (phx) is shaded yellow, surrounding cells in blue. (**D**) Expanded ECM adjacent to the pharynx of a *pxn-2(ju358)* mutant. The pharyngeal cytoskeleton is also abnormal. ecm, extracellular material. Scale bars: 10 μm in A,B; 500 nm in C,D.

2003). *lam-3* RNAi feeding had no effect in the wild-type (N2) background but significantly enhanced lethality and Vab phenotypes when performed on *pxn-2(ju432)* partial loss-of-function mutants (Table 2). *pxn-2(ju432)* also synergized with RNAi for α-integrin (*pat-2*; Table 2). The enhanced sensitivity of *pxn-2* mutants to RNAi for basement membrane components or receptors supports a role for PXN-2 in basement membrane function.

PXN-2 is required to guide specific axons but does not maintain process position

Basement membranes form substrates for outgrowth and guidance of pioneer growth cones. To investigate the role of PXN-2 in neuronal development we examined a panel of neuron types, including cholinergic and GABAergic motoneurons and mechanosensory neurons. Both types of motoneuron extend circumferential commissures across basement membrane to the dorsal cord. Motor axon outgrowth and commissural guidance were mostly normal in *pxn-2* mutants. However, *pxn-2* mutants were strongly defective in the left-right guidance of commissure outgrowth. In the wild type, 17/19 D neuron commissures extend on the right-hand side, whereas in 89% of *ju358* mutants at least one D commissure (of 17 scored) extended on the incorrect, left-hand side (n=53; see Fig. 6A,B); in 13% of *ju358* animals more than four commissures extended incorrectly. Cholinergic DA and DB motoneurons displayed less penetrant handedness defects (not shown). Thus, PXN-2 acts in selective axon guidance decisions but is not essential for axon outgrowth.

Table 2. Synergism of *pxn-2* with laminin and integrin RNAi

Genotype	RNAi	Lethality (%)	Vab adults (%)	*n*
N2	L4440	0.4	0	719
N2	*lam-3*	0.16	0	616
N2	*pat-2*	0.0	47	251
pxn-2(ju432)	L4440	2.8	17.6	216
pxn-2(ju432)	*lam-3*	8.9*	53.2*	158
pxn-2(ju432)	*pat-2*	16*	44	291
pxn-1(ok785)	L4440	0.13	0	765
pxn-1(ok785)	*lam-3*	0.4	0	678
pxn-1(ok785)	*pat-2*	0.0	39*	261
rrf-3	L4440	9.0	0	367
rrf-3	*lam-3*	25.0	0	248
pxn-1(ok785) rrf-3	L4440	17	0	392
pxn-1(ok785) rrf-3	*lam-3*	13*	0	276

Embryonic and larval lethality were scored in the progeny of animals feeding on HT115 bacteria containing either the L4440 empty vector or the *lam-3* RNAi clone. *lam-3* RNAi is not effective in the N2 or *rrf-3* background but strongly enhances *pxn-2(ju432)* lethality and adult Vab phenotypes (*, P<0.05; Fisher's exact test). *pat-2* RNAi causes adult Vab in the N2 background, slightly enhanced lethality in the *pxn-2* background, and reduced Vab phenotypes in the *pxn-1* background (P<0.05).

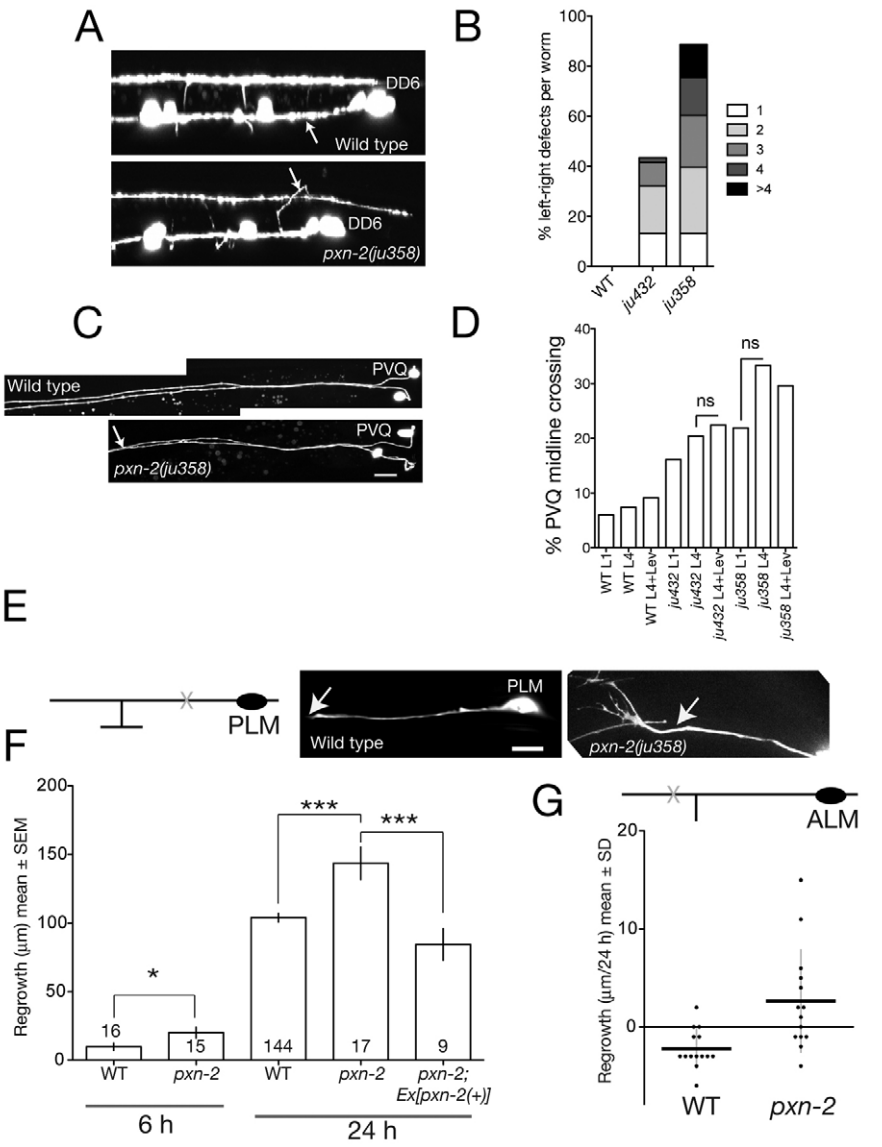

Fig. 6. PXN-2 functions in selective motoneuron axon guidance choice, prevents midline crossing and inhibits touch neuron axon regrowth after laser axotomy. (**A**) In wild-type L1 stage *C. elegans* (P*unc-25*-GFP, *juIs76*), commissures of motoneurons DD2-6 extend on the right-hand side. In *pxn-2(ju358)*, commissures frequently extend on the left-hand side (arrow, DD6 commissure). (**B**) Summary of D neuron commissure handedness defects. The number of commissures that extended incorrectly is shown (*n*>50 per genotype). (**C**) Wild-type PVQ axons are fasciculated in the posterior and separate in the anterior. In *pxn-2(ju358)* animals, PVQ axons inappropriately fasciculate; *oyIs14*. (**D**) *pxn-2* midline crossing defects do not increase during postembryonic development. Quantitation in L1 and L4 stage animals and in L4 animals reared on levamisole (Lev) plates. *n*>45 per group; ns, not significant (Fisher's exact test). (**E**) (Left) Diagram of PLM neuron showing position of axotomy (X). (Right) Images of PLM regrowth 6 hours post-axotomy in wild type and *pxn-2(ju358)*; arrow, site of axotomy. Note the growth-cone-like structure in *pxn-2*. (**F**) Quantitation of PLM (*zdIs5*) regrowth in wild type and *pxn-2(ju358)* at 6 and 24 hours. Sample size is indicated within the columns. *pxn-2* mutants displayed increased regrowth at 6 hours (*, *P*=0.02; Mann-Whitney test). The increased regrowth of *pxn-2* mutants at 24 hours is rescued by the PXN-2(+) transgene *juEx2140* (***, *P*<0.001; ANOVA and Tukey's post-hoc test). (**G**) By 24 hours post-axotomy, the distal process of the ALM neuron retracts slightly in the wild type, whereas in *pxn-2(ju358)* mutants the ALM distal process displays significantly increased regrowth. Dot plot; horizontal lines indicate the mean. *P*=0.003, Mann-Whitney test. Scale bars: 10 µm.

Some basement membrane proteins, such as SPON-1 and DIG-1, act postembryonically to maintain axons in their correct positions (Benard et al., 2006; Woo et al., 2008). To test whether PXN-2 might also maintain axon position, we examined the morphology of PVQ neurons in *pxn-2* mutants. Both *ju432* and *ju358* mutants displayed inappropriate PVQ midline crossing at the L1 stage (Fig. 6C). However, the incidence of PVQ midline crossing did not increase owing to postembryonic 'flip-overs' (Fig. 6D). The postembryonic maintenance function of PXN-2 might be specific to non-neuronal tissues.

PXN-2 inhibits adult axon regrowth after injury

The continued expression of PXN-2 in adult stages prompted us to test whether PXN-2 might influence the ability of mature axons to regrow after injury. We focused on the ALM and PLM mechanosensory (touch) neurons, which display robust regrowth in L4 and adult stages when severed proximally to the synaptic branches, but very little regrowth when severed distally to the synaptic branches (Wu et al., 2007). The developmental outgrowth of touch neurons was largely normal in *pxn-2* partial loss-of-function mutants, although a small percentage of neurons displayed axon overgrowth (not shown). After laser axotomy, the proximal axon of PLM regrew significantly further in *pxn-2(ju358)* mutants than in the wild type at 6 hours (Fig. 6E,F). In the wild type, 1/16 axons formed new growth cones at 6 hours, whereas 7/15 PLM processes had reformed growth cones at 6 hours in *pxn-2* mutants (*P*=0.015, Fisher's exact test). The total regrowth of PLM neurons by 24 hours in *pxn-2* mutants was ~150% that of wild-type PLM neurons; this increased regrowth was fully rescued by the *pxn-2(+)* transgene (Fig. 6E). When severed distally to the synaptic branch, *pxn-2* mutant ALM neurons displayed significantly increased regrowth compared with the wild type (Fig. 6G). Thus, reduced *pxn-2* function can promote regrowth in both regeneration-permissive and regeneration-inhibited situations.

PXN-1 is not essential for development and acts antagonistically to PXN-2

C. elegans encodes a second peroxidasin, PXN-1, which is closely related to PXN-2 (Fig. 1C). *pxn-1* transcriptional reporters were expressed in the epidermis (Fig. 7B), in several classes of neuron, and in vulval and uterine muscles. The deletion *pxn-1(ok785)* is predicted to truncate PXN-1 before the peroxidase domain, and

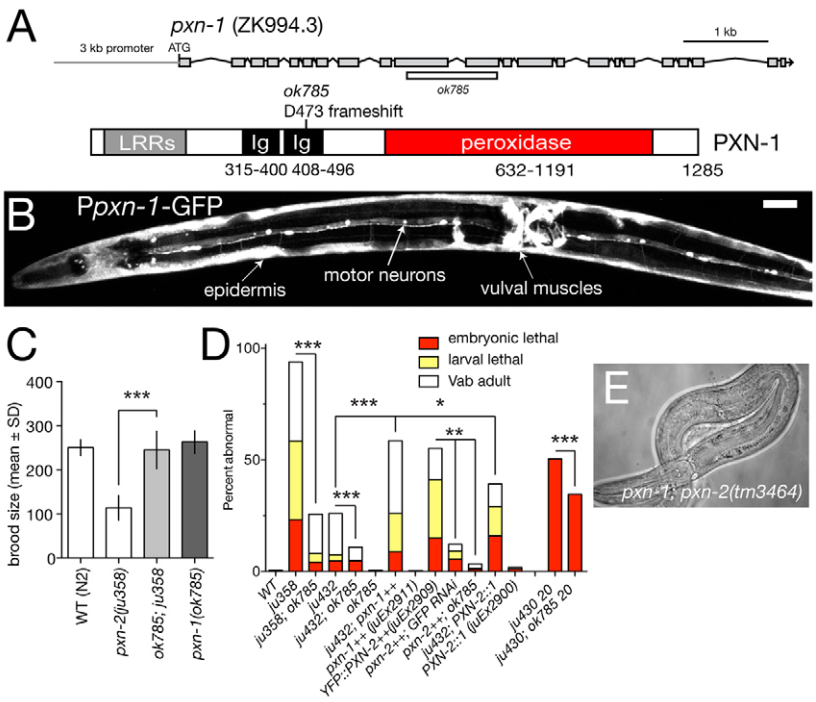

Fig. 7. Antagonistic roles of PXN-1 and PXN-2. (**A**) Structure of the *pxn-1* gene and predicted protein, and location of *ok785* deletion. The *pxn-1* gene structure has not been completely confirmed by cDNA sequencing, but is strongly supported by alignment with the *C. briggsae* genome. (**B**) A P*pxn-1-GFP* transcriptional reporter (*juEx1101*) is expressed in the epidermis, cholinergic motoneurons and vulval muscles. Ventral view of young adult *C. elegans* hermaphrodite. Scale bar: 20 μm. (**C**) *pxn-1(ok785)* suppresses the reduction in brood size of *pxn-2* mutants. *n*=5 broods per genotype; mean ± s.d. ***, *P*<0.001; Student's *t*-test. (**D**) *pxn-1(ok785)* partially suppresses lethal and morphological defects of *pxn-2* mutants, and partly suppresses embryonic lethality of *spon-1(ju430)*. Conversely, transgenes overexpressing wild-type *pxn-1(juEx2911)* significantly enhance both *pxn-2(ju432)* and *pxn-2(ju358)* (not shown). Overexpression of YFP::PXN-2 (*juEx2909*) results in phenotypes resembling PXN-2 loss of function, which are suppressed by *pxn-1* and by RNAi for GFP. Arrays expressing a PXN-2::PXN-1 chimera (*juEx2900*) slightly enhanced *pxn-2(ju432)*; similar results were obtained for the chimera array *juEx2905* (not shown). ***, *P*<0.001; **, *P*<0.01; *, *P*<0.05; Fisher's exact or χ^2 test. (**E**) Approximately 1% of *pxn-2(tm3464); pxn-1(ok785)* animals develop to sterile adults.

should cause a strong loss of function (Fig. 7A). *pxn-1(ok785)* mutants did not display overt defects in epidermal morphogenesis or egg laying. RNAi of *pxn-1* in sensitized backgrounds did not reveal obvious phenotypes (not shown), suggesting that PXN-1 is not essential for basement membrane formation.

We tested whether *pxn-1* might function redundantly with *pxn-2* by analyzing *pxn-1; pxn-2* double mutants. Unexpectedly, *pxn-1(ok785)* significantly suppressed the lethal, morphological and egg-laying defects caused by multiple *pxn-2* alleles (Fig. 7C,D). For example, whereas *ju379* or *tm3464* mutants arrest in embryonic or early L1 stages, *ok785; ju379* and *ok785; tm3464* double mutants arrested at later stages. Approximately 1% of *ok785; tm3464* animals developed to sterile adults (Fig. 7E). As *pxn-1(ok785)* can ameliorate the defects of the deletion allele *pxn-2(tm3464)*, the suppression is unlikely to be due to upregulation of residual functional PXN-2, but suggests that PXN-1 and PXN-2 have antagonistic roles. Indeed, transgenes overexpressing PXN-1 did not cause morphological defects in a wild-type background yet significantly enhanced *pxn-2* mutant phenotypes (Fig. 7D). To further test this antagonistic interaction, we generated transgenes that overexpress YFP::PXN-2 in the wild-type background. These transgenic animals exhibited Pxn-2-like phenotypes that were strongly suppressed by RNAi for GFP (Fig. 7D), suggesting that overexpression of PXN-2 resulted in inhibition of endogenous PXN-2 activity. Consistent with this interpretation, effects of PXN-2 overexpression were fully suppressed by *pxn-1(ok785)* (Fig. 7D). To address the gene specificity of the suppression effects of *pxn-1*, we examined *pxn-1* double mutants with *spon-1* (F-spondin), and found that *pxn-1* significantly suppressed the morphological defects of a *spon-1* mutant (Fig. 7D). *pxn-1* mutants were also slightly resistant to the effects of *pat-2* and *lam-3* RNAi (Table 2).

To investigate the basis of the striking divergence in PXN-1 and PXN-2 functions, we expressed transgenes in which either all or part of the peroxidase domain of PXN-2 had been replaced with that of PXN-1. The resulting YFP-tagged chimeric proteins were expressed at levels comparable to wild-type YFP::PXN-2 (not shown) and did not cause significant defects in a wild-type background (Fig. 7D). Chimera-expressing transgenes failed to rescue *pxn-2*-null mutant phenotypes (not shown) and slightly enhanced the defects of *pxn-2* partial loss-of-function mutants (Fig. 7D). As replacement of the PXN-2 peroxidase domain with that of PXN-1 eliminated *pxn-2* rescue activity, the differences in PXN-1 and PXN-2 function might in part be due to different activities of their peroxidase domains.

DISCUSSION

The functions of peroxidasins have remained enigmatic since their discovery in *Drosophila* (Nelson et al., 1994). The results of our analysis of the developmental and behavioral defects of *pxn-2* mutants are consistent with an essential role for PXN-2 in the formation and maintenance of basement membranes. We further find that reduced PXN-2 function allows increased axonal regeneration after injury in adults, providing the first evidence that the *C. elegans* ECM contributes to an inhibitory environment during axon regrowth.

Although peroxidasins derive their name from the presence of the peroxidase domain, the unusual domain structure of peroxidasins raises the question of whether their peroxidase catalytic activity is important in the ECM, or whether they might have two independent functions. Mutation of the active site histidine in PXN-2 almost eliminated rescuing activity, indicating that catalytic activity is important for PXN-2 developmental functions. A *C. elegans* dual oxidase, BLI-3, has both a peroxidase-dependent function in cuticle cross-linking and a peroxidase-independent role in the generation of reactive oxygen species (Chavez et al., 2009), reflecting the presence of a second catalytic oxidase domain in the protein. As peroxidasins have only a single catalytic domain, any peroxidase-independent functions presumably involve the LRR or Ig domains, which we also find are required for PXN-2 function. Peroxidasins contain a highly conserved cysteine-rich motif in their C-termini that is related to the Von Willebrand factor type C domain and is thought to promote trimerization (Nelson et al., 1994). Strikingly, missense alteration of

a semi-conserved glycine (G1314), as in the strong *pxn-2* allele *ju379*, almost completely abolished PXN-2 function, supporting the hypothesis that the C-terminus of peroxidasins is important for function. Together, our data show that peroxidasins are functional peroxidases that contribute to ECM formation via multiple domains.

pxn-2 mutants display disorganization of ECM and striking expansion of matrix material. Similar stacking of basement-membrane-like structures has been observed in some *C. elegans* ECM mutants, such as *dig-1* (Benard et al., 2006), whereas expansion of ECM is occasionally observed in laminin αA (*epi-1*) mutants (Huang et al., 2003). PXN-2 might promote the consolidation of a less structured ECM precursor into mature basement membranes. Taken together with the late onset of *pxn-2* defects, these results suggest that PXN-2 plays a restricted role in late matrix assembly or consolidation.

As with other peroxidases, peroxidasin can catalyze the formation of dityrosine cross-links in vitro. Many extracellular matrices, such as cuticles or egg shells, are strengthened by peroxidase-catalyzed dityrosine cross-links (Andersen, 1964; Konstandi et al., 2005; Wong and Wessel, 2008). In *C. elegans*, dityrosine cross-linking is required for cuticle integrity and is catalyzed by the dual oxidase-peroxidase Ce-Duox1/BLI-3 and the peroxidase MLT-7 (Edens et al., 2001; Thein et al., 2009). Although expressed in epidermis, PXN-2 does not appear to cross-link cuticle, but might play an analogous role in the basement membrane. Dityrosine cross-linking has been proposed as a function for peroxidasins in basement membranes, yet dityrosine itself has not thus far been directly detected in basement membranes. It remains possible that peroxidasins provide oxidants for other kinds of post-translational modifications. Vertebrate fibrillar collagens are extensively cross-linked by lysyl oxidase (Robins, 2007); however, *C. elegans* lacks fibrillar collagens (Myllyharju and Kivirikko, 2004). An important future goal is to identify the in vivo substrates of PXN-2 and other peroxidasins.

PXN-2 is essential for late steps in basement membrane formation, and specifically where mechanically strong attachment between tissues and ECM is required. *pxn-2* mutants display progressive dystrophy of the pharynx, reminiscent of fibulin (*fbl-1*) mutants (Muriel et al., 2005). However, *pxn-2* mutants do not display defects in gonadal development or integrity, which are found in laminin or fibulin mutants (Hesselson et al., 2004; Kubota et al., 2004). Pharyngeal muscles are likely to require a mechanically strong basement membrane to exert force against during contraction. By contrast, basement membranes, such as those of the intestine or gonad, might have a lesser need to withstand muscle contractions and thus do not require PXN-2.

We find that loss of *pxn-2* function influences the ability of mature neurons to regenerate after injury. PXN-2 might interact directly with axonal receptors during axon navigation. Alternatively, PXN-2 could play an indirect role in that aberrant ECM in *pxn-2* mutants might constitute a more permissive environment for regrowth. Extensive studies of vertebrate axon regeneration have shown that ECM components can be regrowth promoting or inhibiting (Busch and Silver, 2007). Our findings raise the possibility that mammalian peroxidasins are extracellular inhibitors of regrowth. Inhibitors of peroxidasin catalytic activity could have therapeutic benefits in situations of axon injury.

Most animals express multiple peroxidasins, either as products of multiple peroxidasin genes or from alternative splicing of a single gene. Gene duplication can result in an initial redundancy of function, followed by subfunctionalization if the duplicated genes take on distinct roles in different tissues or at different times (Lynch and Force, 2000; Tvrdik and Capecchi, 2006). Although the two *C. elegans* peroxidasins are closely related, our data suggest that *pxn-1* and *pxn-2* have become subfunctionalized. PXN-1 might have peroxidase-independent functions that could be mediated by truncated proteins made in *ok785* mutants, yet RNAi of *pxn-1* failed to reveal developmental phenotypes. Partial redundancy of function should be reflected in phenotypic enhancement in a double mutant, yet *pxn-1; pxn-2* double mutants display suppression of *pxn-2* mutant phenotypes. *pxn-1* loss of function also suppressed *spon-1* partial loss of function, consistent with PXN-1 acting as a negative regulator of basement membrane assembly or function.

Elevated expression of peroxidases, such as MPO, during inflammation or tissue injury can degrade ECM as a result of an overproduction of extracellular oxidants and consequent inactivation of protease inhibitors (Wang et al., 2007). PXN-1 could play an analogous regulatory role in the *C. elegans* matrix. Intriguingly, loss of *pxn-1* function can enhance neurodegenerative phenotypes caused by overexpression of the microtubule-binding protein tau (MAPT) in *C. elegans*, implying that PXN-1 protects against neurodegeneration (Kraemer et al., 2006). Further work will be required to determine whether the neuroprotective effects of PXN-1 are related to its role in regulating the ECM.

Acknowledgements

We thank Mei Ding and Wei-Meng Woo for collaboration in the elongation screen; Lizhen Chen for constructing the *zdIs5* rescue strain; members of our labs for help and advice; Alan Zahler, Manny Ares and Emily Troemel for discussions; and Mark Ellisman (National Center for Microscopy and Imaging Research, UCSD) and Marilyn Farquhar (Department of Cellular and Molecular Medicine, UCSD) for electron microscopy resources. Deletion alleles were generously provided by the *C. elegans* Gene Knockout Consortium (*ok785*) and the Japan National BioResource Project (*tm3464*). We thank B. Vogel (University of Maryland) for *rhIs23*. Z.W. and A.G. are Associates and Y.J. is an Investigator of the Howard Hughes Medical Institute. This work was supported by NIH award F32 GM090652 to C.A.G. and R01 awards GM54657 and NS57317 to A.D.C. Deposited in PMC for release after 6 months.

Competing interests statement

The authors declare no competing financial interests.

Supplementary material

Supplementary material for this article is available at
http://dev.biologists.org/lookup/suppl/doi:10.1242/dev.049189/-/DC1

References

Alfonso, T. B. and Jones, B. W. (2002). gcm2 promotes glial cell differentiation and is required with glial cells missing for macrophage development in Drosophila. *Dev. Biol.* **248**, 369-383.

Andersen, S. O. (1964). The cross-links in resilin identified as dityrosine and trityrosine. *Biochim. Biophys. Acta* **93**, 213-215.

Aratani, Y., Koyama, H., Nyui, S., Suzuki, K., Kura, F. and Maeda, N. (1999). Severe impairment in early host defense against *Candida albicans* in mice deficient in myeloperoxidase. *Infect. Immunol.* **67**, 1828-1836.

Benard, C. Y., Boyanov, A., Hall, D. H. and Hobert, O. (2006). DIG-1, a novel giant protein, non-autonomously mediates maintenance of nervous system architecture. *Development* **133**, 3329-3340.

Busch, S. A. and Silver, J. (2007). The role of extracellular matrix in CNS regeneration. *Curr. Opin. Neurobiol.* **17**, 120-127.

Chavez, V., Mohri-Shiomi, A. and Garsin, D. A. (2009). Ce-Duox1/BLI-3 generates reactive oxygen species as a protective innate immune mechanism in *Caenorhabditis elegans*. *Infect. Immunol.* **77**, 4983-4989.

Cheng, G., Salerno, J. C., Cao, Z., Pagano, P. J. and Lambeth, J. D. (2008). Identification and characterization of VPO1, a new animal heme-containing peroxidase. *Free Radic. Biol. Med.* **45**, 1682-1694.

Chisholm, A. D. and Hardin, J. (2005). Epidermal morphogenesis. *WormBook*, http://www.wormbook.org.

Clark, S. G. and Chiu, C. (2003). *C. elegans* ZAG-1, a Zn-finger-homeodomain protein, regulates axonal development and neuronal differentiation. *Development* **130**, 3781-3794.

Daiyasu, H. and Toh, H. (2000). Molecular evolution of the myeloperoxidase family. *J. Mol. Evol.* **51**, 433-445.

Dixon, S. J., Alexander, M., Fernandes, R., Ricker, N. and Roy, P. J. (2006). FGF negatively regulates muscle membrane extension in *Caenorhabditis elegans*. *Development* **133**, 1263-1275.
Edens, W. A., Sharling, L., Cheng, G., Shapira, R., Kinkade, J. M., Lee, T., Edens, H. A., Tang, X., Sullards, C., Flaherty, D. B. et al. (2001). Tyrosine cross-linking of extracellular matrix is catalyzed by Duox, a multidomain oxidase/peroxidase with homology to the phagocyte oxidase subunit gp91phox. *J. Cell Biol.* **154**, 879-891.
Furtmuller, P. G., Zederbauer, M., Jantschko, W., Helm, J., Bogner, M., Jakopitsch, C. and Obinger, C. (2006). Active site structure and catalytic mechanisms of human peroxidases. *Arch. Biochem. Biophys.* **445**, 199-213.
George, S. E., Simokat, K., Hardin, J. and Chisholm, A. D. (1998). The VAB-1 Eph receptor tyrosine kinase functions in neural and epithelial morphogenesis in *C. elegans*. *Cell* **92**, 633-643.
Gupta, M. C., Graham, P. L. and Kramer, J. M. (1997). Characterization of alpha1(IV) collagen mutations in *Caenorhabditis elegans* and the effects of alpha1 and alpha2(IV) mutations on type IV collagen distribution. *J. Cell Biol.* **137**, 1185-1196.
Hansson, M., Olsson, I. and Nauseef, W. M. (2006). Biosynthesis, processing, and sorting of human myeloperoxidase. *Arch. Biochem. Biophys.* **445**, 214-224.
Hart, A. C. (2006). Behavior. *WormBook*, http://www.wormbook.org.
Heinecke, J. W., Li, W., Daehnke, H. L., 3rd and Goldstein, J. A. (1993). Dityrosine, a specific marker of oxidation, is synthesized by the myeloperoxidase-hydrogen peroxide system of human neutrophils and macrophages. *J. Biol. Chem.* **268**, 4069-4077.
Hesselson, D., Newman, C., Kim, K. W. and Kimble, J. (2004). GON-1 and fibulin have antagonistic roles in control of organ shape. *Curr. Biol.* **14**, 2005-2010.
Hobert, O. (2002). PCR fusion-based approach to create reporter gene constructs for expression analysis in transgenic *C. elegans*. *Biotechniques* **32**, 728-730.
Hobert, O., Mori, I., Yamashita, Y., Honda, H., Ohshima, Y., Liu, Y. and Ruvkun, G. (1997). Regulation of interneuron function in the *C. elegans* thermoregulatory pathway by the *ttx-3* LIM homeobox gene. *Neuron* **19**, 345-357.
Homma, S., Shimada, T., Hikake, T. and Yaginuma, H. (2009). Expression pattern of LRR and Ig domain-containing protein (LRRIG protein) in the early mouse embryo. *Gene Expr. Patterns* **9**, 1-26.
Hong, L., Elbl, T., Ward, J., Franzini-Armstrong, C., Rybicka, K. K., Gatewood, B. K., Baillie, D. L. and Bucher, E. A. (2001). MUP-4 is a novel transmembrane protein with functions in epithelial cell adhesion in *Caenorhabditis elegans*. *J. Cell Biol.* **154**, 403-414.
Horikoshi, N., Cong, J., Kley, N. and Shenk, T. (1999). Isolation of differentially expressed cDNAs from p53-dependent apoptotic cells: activation of the human homologue of the Drosophila peroxidasin gene. *Biochem. Biophys. Res. Commun.* **261**, 864-869.
Huang, C. C., Hall, D. H., Hedgecock, E. M., Kao, G., Karantza, V., Vogel, B. E., Hutter, H., Chisholm, A. D., Yurchenco, P. D. and Wadsworth, W. G. (2003). Laminin alpha subunits and their role in *C. elegans* development. *Development* **130**, 3343-3358.
Huang, X., Cheng, H. J., Tessier-Lavigne, M. and Jin, Y. (2002). MAX-1, a novel PH/MyTH4/FERM domain cytoplasmic protein implicated in netrin-mediated axon repulsion. *Neuron* **34**, 563-576.
Hudson, M. L., Kinnunen, T., Cinar, H. N. and Chisholm, A. D. (2006). *C. elegans* Kallmann syndrome protein KAL-1 interacts with syndecan and glypican to regulate neuronal cell migrations. *Dev. Biol.* **294**, 352-365.
Ihalin, R., Loimaranta, V. and Tenovuo, J. (2006). Origin, structure, and biological activities of peroxidases in human saliva. *Arch. Biochem. Biophys.* **445**, 261-268.
Jacquet, A., Garcia-Quintana, L., Deleersnyder, V., Fenna, R., Bollen, A. and Moguilevsky, N. (1994). Site-directed mutagenesis of human myeloperoxidase: further identification of residues involved in catalytic activity and heme interaction. *Biochem. Biophys. Res. Commun.* **202**, 73-81.
Johansson, M. W., Lind, M. I., Holmblad, T., Thornqvist, P. O. and Soderhall, K. (1995). Peroxinectin, a novel cell adhesion protein from crayfish blood. *Biochem. Biophys. Res. Commun.* **216**, 1079-1087.
Johansson, M. W., Patarroyo, M., Oberg, F., Siegbahn, A. and Nilsson, K. (1997). Myeloperoxidase mediates cell adhesion via the alpha M beta 2 integrin (Mac-1, CD11b/CD18). *J. Cell Sci.* **110**, 1133-1139.
Kamath, R. S., Fraser, A. G., Dong, Y., Poulin, G., Durbin, R., Gotta, M., Kanapin, A., Le Bot, N., Moreno, S., Sohrmann, M. et al. (2003). Systematic functional analysis of the *Caenorhabditis elegans* genome using RNAi. *Nature* **421**, 231-237.
Konstandi, O. A., Papassideri, I. S., Stravopodis, D. J., Kenoutis, C. A., Hasan, Z., Katsorchis, T., Wever, R. and Margaritis, L. H. (2005). The enzymatic component of Drosophila melanogaster chorion is the Pxd peroxidase. *Insect Biochem. Mol. Biol.* **35**, 1043-1057.
Kraemer, B. C., Burgess, J. K., Chen, J. H., Thomas, J. H. and Schellenberg, G. D. (2006). Molecular pathways that influence human tau-induced pathology in *Caenorhabditis elegans*. *Hum. Mol. Genet.* **15**, 1483-1496.
Kramer, J. M. (2005). Basement membranes. *WormBook*, http://www.wormbook.org.
Kubota, Y., Kuroki, R. and Nishiwaki, K. (2004). A fibulin-1 homolog interacts with an ADAM protease that controls cell migration in *C. elegans*. *Curr. Biol.* **14**, 2011-2018.
Lehrer, R. I. and Cline, M. J. (1969). Leukocyte myeloperoxidase deficiency and disseminated candidiasis: the role of myeloperoxidase in resistance to Candida infection. *J. Clin. Invest.* **48**, 1478-1488.
Lynch, M. and Force, A. (2000). The probability of duplicate gene preservation by subfunctionalization. *Genetics* **154**, 459-473.
Mitchell, M. S., Kan-Mitchell, J., Minev, B., Edman, C. and Deans, R. J. (2000). A novel melanoma gene (MG50) encoding the interleukin 1 receptor antagonist and six epitopes recognized by human cytolytic T lymphocytes. *Cancer Res.* **60**, 6448-6456.
Muriel, J. M., Dong, C., Hutter, H. and Vogel, B. E. (2005). Fibulin-1C and Fibulin-1D splice variants have distinct functions and assemble in a hemicentin-dependent manner. *Development* **132**, 4223-4234.
Myllyharju, J. and Kivirikko, K. I. (2004). Collagens, modifying enzymes and their mutations in humans, flies and worms. *Trends Genet.* **20**, 33-43.
Nelson, R. E., Fessler, L. I., Takagi, Y., Blumberg, B., Keene, D. R., Olson, P. F., Parker, C. G. and Fessler, J. H. (1994). Peroxidasin: a novel enzyme-matrix protein of Drosophila development. *EMBO J.* **13**, 3438-3447.
O'Brien, P. J. (2000). Peroxidases. *Chem. Biol. Interact.* **129**, 113-139.
Olofsson, B. and Page, D. T. (2005). Condensation of the central nervous system in embryonic Drosophila is inhibited by blocking hemocyte migration or neural activity. *Dev. Biol.* **279**, 233-243.
Priess, J. R. and Hirsh, D. I. (1986). *Caenorhabditis elegans* morphogenesis: the role of the cytoskeleton in elongation of the embryo. *Dev. Biol.* **117**, 156-173.
Rees, M. D., Kennett, E. C., Whitelock, J. M. and Davies, M. J. (2008). Oxidative damage to extracellular matrix and its role in human pathologies. *Free Radic. Biol. Med.* **44**, 1973-2001.
Robins, S. P. (2007). Biochemistry and functional significance of collagen cross-linking. *Biochem. Soc. Trans.* **35**, 849-852.
Ruf, J. and Carayon, P. (2006). Structural and functional aspects of thyroid peroxidase. *Arch. Biochem. Biophys.* **445**, 269-277.
Schafer, W. F. (2006). Genetics of egg-laying in worms. *Annu. Rev. Genet.* **40**, 487-509.
Stofanko, M., Kwon, S. Y. and Badenhorst, P. (2008). A misexpression screen to identify regulators of Drosophila larval hemocyte development. *Genetics* **180**, 253-267.
Thein, M. C., Winter, A. D., Stepek, G., McCormack, G., Stapleton, G., Johnstone, I. L. and Page, A. P. (2009). Combined extracellular matrix cross-linking activity of the peroxidase MLT-7 and the dual oxidase BLI-3 is critical for post-embryonic viability in *Caenorhabditis elegans*. *J. Biol. Chem.* **284**, 17549-17563.
Tindall, A. J., Pownall, M. E., Morris, I. D. and Isaacs, H. V. (2005). Xenopus tropicalis peroxidasin gene is expressed within the developing neural tube and pronephric kidney. *Dev. Dyn.* **232**, 377-384.
Tvrdik, P. and Capecchi, M. R. (2006). Reversal of Hox1 gene subfunctionalization in the mouse. *Dev. Cell* **11**, 239-250.
Vogel, B. E. and Hedgecock, E. M. (2001). Hemicentin, a conserved extracellular member of the immunoglobulin superfamily, organizes epithelial and other cell attachments into oriented line-shaped junctions. *Development* **128**, 883-894.
Wang, J. and Slungaard, A. (2006). Role of eosinophil peroxidase in host defense and disease pathology. *Arch. Biochem. Biophys.* **445**, 256-260.
Wang, Y., Rosen, H., Madtes, D. K., Shao, B., Martin, T. R., Heinecke, J. W. and Fu, X. (2007). Myeloperoxidase inactivates TIMP-1 by oxidizing its N-terminal cysteine residue: an oxidative mechanism for regulating proteolysis during inflammation. *J. Biol. Chem.* **282**, 31826-31834.
Weimer, R. M. (2006). Preservation of *C. elegans* tissue via high-pressure freezing and freeze-substitution for ultrastructural analysis and immunocytochemistry. *Methods Mol. Biol.* **351**, 203-221.
Wicks, S. R., Yeh, R. T., Gish, W. R., Waterston, R. H. and Plasterk, R. H. (2001). Rapid gene mapping in *Caenorhabditis elegans* using a high density polymorphism map. *Nat. Genet.* **28**, 160-164.
Williams, B. D. and Waterston, R. H. (1994). Genes critical for muscle development and function in *Caenorhabditis elegans* identified through lethal mutations. *J. Cell Biol.* **124**, 475-490.
Wong, J. L. and Wessel, G. M. (2008). Free-radical crosslinking of specific proteins alters the function of the egg extracellular matrix at fertilization. *Development* **135**, 431-440.
Woo, W. M., Berry, E. C., Hudson, M. L., Swale, R. E., Goncharov, A. and Chisholm, A. D. (2008). The *C. elegans* F-spondin family protein SPON-1 maintains cell adhesion in neural and non-neural tissues. *Development* **135**, 2747-2756.
Wu, Z., Ghosh-Roy, A., Yanik, M. F., Zhang, J. Z., Jin, Y. and Chisholm, A. D. (2007). *Caenorhabditis elegans* neuronal regeneration is influenced by life stage, ephrin signaling, and synaptic branching. *Proc. Natl. Acad. Sci. USA* **104**, 15132-15137.
Zamocky, M., Jakopitsch, C., Furtmuller, P. G., Dunand, C. and Obinger, C. (2008). The peroxidase-cyclooxygenase superfamily: reconstructed evolution of critical enzymes of the innate immune system. *Proteins* **72**, 589-605.